SCIENCE AND TECHNOLOGY OF WELDING AND JOINING, 2017
https://doi.org/10.1080/13621718.2017.1341363

The Institute of Materials, Minerals and Mining

Taylor & Francis
Taylor & Francis Group

Effects of thread interruptions on tool pins in friction stir welding of AA6061

Md. Reza-E-Rabby[a], Wei Tang[b] and Anthony P. Reynolds[a,c]

[a]Pacific Northwest National Laboratory, Richland, WA, USA; [b]Oak Ridge National Laboratory, Oak Ridge, TN, USA; [c]Department of Mechanical Engineering, University of South Carolina, Columbia, SC, USA

ABSTRACT

In this work, effects of pin thread and thread interruptions (flats) on weld quality and process response parameters during friction stir welding (FSW) of 6061 aluminium alloy were quantified. Otherwise, identical smooth and threaded pins with zero to four flats were adopted for FSW. Weldability and process response variables were examined. Results showed that threads with flats significantly improved weld quality and reduced in-plane forces. A three-flat threaded pin led to production of defect-free welds under all examined welding conditions. Spectral analyses of in-plane forces and weld cross-sectional analysis were performed to establish correlation among pin flats, force dynamics and defect formation. The lowest in-plane force spectra amplitudes were consistently observed for defect-free welds.

ARTICLE HISTORY
Received 27 April 2017
Accepted 6 June 2017

KEYWORDS
Friction stir welding; unthreaded pin; threaded pin; flats; in-plane forces

Introduction

In friction stir welding (FSW) [1], a non-consumable rotating tool causes solid state bonding between adjacent materials by severe plastic deformation, viscous dissipation and subsequent consolidation of material during its traverse. Among the primary process control parameters, the geometric variability of the non-consumable tool is essentially infinite. Typically, adopted geometries are based on experience with chosen weld material properties, thickness, and implemented welding speed/rotational speed. Of the tool geometric variables, pin thread form and features (flats/flutes) are often considered to be most influential parameters to control weld quality in thick plate since downward material movement is driven by these helical features. [2–4] The shoulder-dominated plastic deformation diminishes with increasing weld depth in a thick section plate [5] regardless of shoulder geometric configurations (concave, flat scrolled or convex shoulders with/without tool tilting angle) [6–8]. Moreover, with the development of stationary shoulder tooling, the effect of uniform heat generation and material transport are being driven by the rotating pin only, which also showed some promises in improving weld quality by homogenising through thickness material properties in the weld [9–12]. Therefore, effective pin design is a critical issue in the FSW community.

Previously, selection of FSW tool geometries and pin features was mostly on the basis of intuition or empirical knowledge [13]. Systematic tool design concepts are scantily available in the open literature. Nevertheless, an excellent experimental effort has been made by Hattingh et al. [14] who investigated the effect of tool geometries on welding force and mechanical properties of friction stir welds of AA5083 to understand the key characteristics of FSW process in light of the interaction of tooling and welding parameters. Systematic variation in number of flutes, flute depth and angles, pin diameter and taper angle, and thread pitch were reported with the reaction forces on the pin and correlated with the resulting tensile strength. However, for a subset of process windows, taper three fluted pin was reported to be optimum with high welding efficiency in their study. In other studies, randomly chosen pin geometric shapes, for example square/triangular/hexagonal/octagonal prismatic, taper square/octagonal were also studied to identify the effectiveness of these pin geometries for successful friction stir welds [15–18]. In consequence, there are claims for local optimum tool geometric configurations under a range of examined welding parameters.

Interrupting the pin thread with flats/flutes was also found to be beneficial in FSW by many researchers for effective material flow around the tool as supported by experimental investigations [8,14,19–21]. The microstructural observations of weld material in the front vicinity of pin suggest the trapping of the materials in the thread and subsequent release near flats after experiencing one or more rotations along with the pin as revealed from ultrafine grains with texture and their orientation from stop action FSW process [22]. The disrupted material flow by threaded and three

CONTACT Md. Reza-E-Rabby md.reza-e-rabby@pnnl.gov Pacific Northwest National Laboratory, 902 Battelle Boulevard, P.O. Box 999, MSIN K2-03, Richland, WA 99352, USA

Table 1. Applied process control parameters studied in this paper.

Welding parameter set:	I	II	III	IV	V	VI
Rotation rate (rev min^{-1}):	160	200	240	240	320	400
Welding speed (mm min^{-1}):	102	102	102	203	203	203

flatted pin was also suggested from the observation of two additional weaker rings or smaller peaks within the major microstructural band in every third of the advance per revolution [5,22]. However, eccentric rotation of an off-centred tool may cause reverse shear orientation in texture possibly due to the reversal of the response force components associated with variation in welding speed [5].

The FSW process forces might be correlated with quality of welds during FSW. Unfortunately, results and observations regarding tool parameters' effect on process forces (in-plane reaction forces) are scarcely available in the open literature. Colegrove and Shercliff [23] compared the transverse force on trivex and triflute pins; the trivex pin was found to reduce the downward force and traverse force (X-axis force) in both experimental and numerical analysis. However, the use of isothermal material properties caused under-predicted traverse force in their computational analysis. Trimble et al. [24] experimentally and numerically investigated the force generation in FSW on smooth and threaded cylindrical pins. They reported that the maximum vertical forces were evident during the plunging sequence and reduced significantly (35% reduction) during translation sequence. Moreover, lower maximum vertical and translational (X-axis) forces were also reported for threaded pin compared with smooth pins. Balasubramanian et al. [25] attempted to understand the material flow phenomena using the tool feedback forces. The orientations of resultant forces (polar plot of in-plane reaction for single cycle) were observed to be shifted towards the retreating side and trailing edge for welds with wormhole defects which are generally observed on the advancing side.

The present study deals with the quantification of the effects of pin thread form and thread features (flats) on friction stir weldability and process response variables. The flat numbers on unthreaded and threaded pins were varied systematically to perform FSW of an aluminium alloy (AA6061-T651). The behaviour of in-plane reaction forces and force dynamics was analysed to improve the understanding of the FSW process by correlating tool features, feedback forces and defect formation.

Experimental methods

FSW was performed on AA6061-T651 using cylindrical tool pins with various features. AA6061 was chosen for its wide FSW process window: good quality welds can normally be produced over a wide range of chosen parameters. Hence pin feature effects can be examined in a large processing window. The nominal composition of AA6061 is: 1.2 wt-% Mg, 0.5 wt-% Si, 0.33 wt-% Fe, 0.28 wt-% Cu, 0.17 wt-% Cr, balance Al. The solidus and the solution heat treatment temperatures of AA6061 are 582°C and 530°C, respectively. Tool shoulder geometry and dimension were kept constant, while pin features were varied in being either unthreaded (smooth) or threaded and varying the number of flats. This tool variation was facilitated by constructing the tools in two pieces with separate pins and shoulders. The shoulder dimensions were 25.4 mm diameter, single scroll with a scroll pitch of 2.54 mm/revolution. The geometric dimensions of the pins were 12.5 mm in length and 15.9 mm in diameter. One, two and four flats were machined on unthreaded pins. For a threaded pin (2.12 mm pitch/12 threads per inch), threads were interrupted by machining one (1), two (2), three (3) and four (4) flats. The dimension of this thread pitch was selected based on previous experimental evaluation for its ability to minimise wormhole defects in FSW on various aluminium alloys. [26] For both threaded and unthreaded pins, the no-flat condition was also examined in this study. Two, three and four flats were placed 180°, 120° and 90° apart, respectively. All the flats were machined to a depth of 1.35 mm, which is just beyond the depth of the thread root. The welding tools used in this study were made of H13 steel. All tool components were austenitised for 20 min at 980°C followed by quenching in oil to achieve hardness of 45–48 HRC. Q4 The thickness of weld material is 25.6 mm. Therefore, all the welds were partial penetration bead on plates which facilitate avoidance of the effect of backing plate to maintain similar thermal boundary condition during welding. The weld parameters used for this study are summarised in Table 1.

Welding was performed on the University of South Carolina (USC) FSW process development system using forge force control mode. For each weld parameter set, forge force (Z-axis force) was adjusted to maintain similar depth of penetration based on observed contact conditions between the shoulder and top surface of the welded plate. Temperature during welding was recorded using a k-type thermocouple spot welded into the pin at mid depth in between shoulder and pin tip along the axis of rotation. Oxidation was removed from the top surface of each workpiece using a hand grinder with a nylon bristle disc. Predrilled holes (14.28 mm diameter and 12.2 mm depth) were made at the weld starting point to ease plunging. Plates were clamped by finger clamps on a steel back plate. All welds were performed at 0° spindle tilt angle. In-plane reaction forces on FSW conventional X-axis

were recorded from the signal produced from the piston pressure transducer on the *X*-axis hydraulic actuator. *Y*-axis forces were obtained from forge force load cells in the spindle carriage. The definitions of the *X*-axis, *Y*-axis forces and their orientations are elaborated in the section 'Influence of flats on applied forge force and in-plane reaction forces'. Tool torque was obtained from a torque transducer attached to the spindle. Weld power was calculated from torque feedback and tool rotation rate.

Metallographic specimens were machined using an abrasive water jet at a location of 125 mm from the start of each weld. Standard metallographic procedures were followed for grinding and polishing steps to prepare the specimens for macro- and microstructural investigations. Specimens were chemically etched using Keller's reagent (2.5 vol.-% HNO_3, 1.5 vol.-% HCl, 1 vol.-% HF and balance distilled water) for macro- and microstructural observation using an Olympus PME 3 optical microscope.

Results

Investigation of defect formation of AA6061 during FSW with flats in pins

Figure 1(a–b) shows the transverse macro-sections of the welds with unthreaded pin (Figure 1(a)) and threaded pin (Figure 1(b)) having different flat numbers. In each macro-section, the advancing side is on the left. It is interesting to note that the wormhole defects were not eliminated with the application of flats to the unthreaded pin, as shown in Figure 1(a). However, the size of the wormhole defects is mostly dependent on welding parameters, as shown in Figure 1(c). In the case of unthreaded pin without flats, defect area increases with increasing tool rotational speed (circular symbol in Figure 1(c)). Contrarily for the flatted pins, defect content decreases with increasing tool rotation rate for similar traverse speed (see Figure 1(c)). Moreover, two and one flatted pins produce higher defect content in the welds at respectively 102 and 203 mm min^{-1} welding speed. Nevertheless, the defects are localised to the near root region on the advancing side, as the number of flats is increased without altering the volume of wormholes. This indicates the role of higher flat numbers in improving the material transport around the pin while also illustrating that helical features are necessary to produce downward flow which eliminates root defects. On the other hand, macro-structural investigations revealed no wormhole defect, but surface breaking defects for several of the welds performed with threaded pins had different flat numbers (Figure 1(b)). Figure 2 (a) and (b) shows two representative microscopic defects in weld cross-sections near weld crown. Interestingly, pin with three

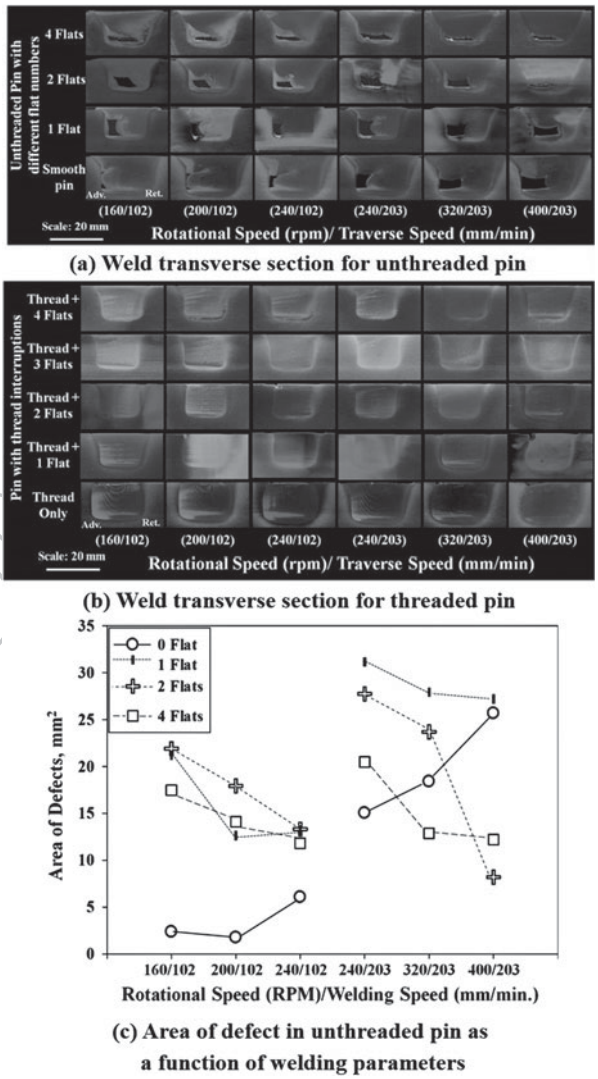

Figure 1. Weld transverse macro-cross-sections for welding with pin having different flat numbers and defect area plots as a function of weld parameters.

flats produced the best results based on the macro- and microscopic examination.

It was observed that for many of the welding conditions, upon pin retraction, the unthreaded pins had some material adhering to the trailing side of the flat. On the other hand, the threaded pin with flats was found free from this adhesion. Examples are shown in Figure 3 (unthreaded and threaded pin with flats are presented in the left and the right images, respectively). This phenomenon of material adhesion might have effect on tool reactions and will be explained by correlating tool design and in-plane reaction forces on the pin in the 'Discussion' section.

In summary, it was observed from macro- and microstructural evaluation that completely defect-free welds were produced with the threaded pin having three flats. Hence, the performance of the cylindrical shape pin having thread pitch of 2.12 mm and three flats was unique for this given set of weld parameters in producing defect-free welds on this particular weld

Colour online, B/W in print

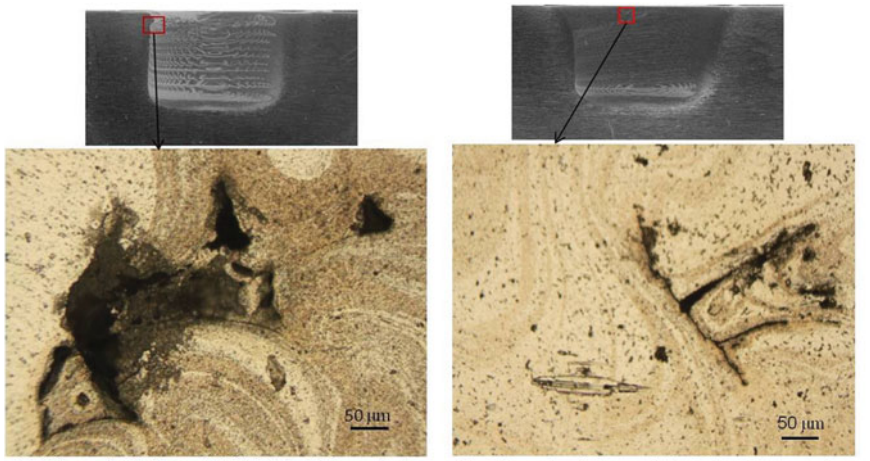

Figure 2. Typical microscopic defect near weld crown with two different tool features and welding parameters.

Colour online, B/W in print

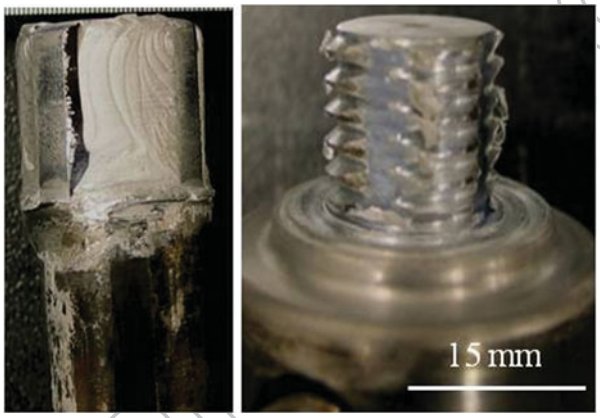

Figure 3. Unthreaded pin (left) and threaded pin (right) showing material adhering to flats (or not).

material. It may be surmised that for the pin geometry used, the optimum balance of rotational transport and vertical transport of material is achieved for the threaded and three flats tool.

Influence of flats on applied forge force and in-plane reaction forces

It was mentioned in the experimental procedure section that force control mode was used for this study; therefore, the forge force was adjusted to obtain similar contact condition between weld materials and tool shoulder based on the pin feature and welding parameters. The required forge forces as a function of welding parameters (rotational and welding speed) are shown in the form of histogram for different flat numbers in Figure 4: (i) unthreaded pins in Figure 4(a) and (ii) threaded pins in Figure 4(b). It is interesting to note from Figure 4(a) that, required forge force is higher for higher flat numbers for similar welding condition in case of unthreaded pins for up to 240 rev min^{-1} rotational speed and minute difference was observed at 320 and 400 rev min^{-1}. However, threaded-only pin (no flats) always required higher forge force compared to any other pin features for similar welding parameters (see Figure 4(b)). This is conceptually understandable, since materials in the threaded channel are to be transported in the downward direction continuously (no interruption for threaded-only pin) resulting in an upward thrust on tool for a right-hand-threaded pin rotating in counter-clock wise direction. Hence, additional forge force is required in this case.

Tool feedback forces were analysed to reveal effect of flats on in-plane reaction forces during FSW. Figure 5 (a–e) shows the polar plots of average in plane reaction forces for pins with different flat numbers. This polar plot is set up with the convention shown in Figure 5(f), where force exerted by the workpiece that impedes the motion of tool in the welding direction is defined as positive X-axis force. Positive Y-axis force acts perpendicular to X direction towards the advancing side from the retreating side. It is observed in polar plots of Figure 5 that, the unthreaded pin produces the largest in plane forces (highest resultant magnitude) in all weld conditions and flat numbers compared to threaded pin. It is also revealed from Figure 5(a–e) that, the range of orientation (θ) of the in-plane resultant force does not vary much for unthreaded pins; however, the average range of orientation decreased with increasing flat numbers. On the contrary, the range of θ is the highest for no flats and decreases with increasing flat number for threaded pins (although, the spread for three and four flats is similar). Table 2 summarises the spread of the orientation of resultants for different pin features (absence/presence of thread) and flat numbers. While considering similar welding parameters, it is worth to note for the unthreaded pin that, increasing flat number led to orientation range of the resultant force to be decreased. On the other hand, orientation of the resultant increases with increasing flat number for threaded pin. The presence of three and four flats (Figure 5(d,e)) continues the trend of narrowing θ around a value near

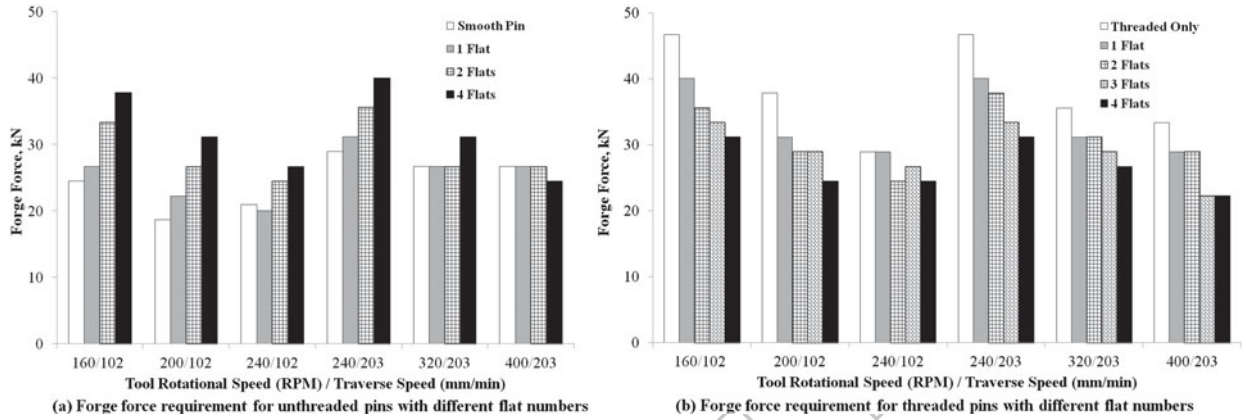

Figure 4. Applied forge force during FSW process on the basis of maintaining similar contact condition between weld materials and tool shoulder due to variation of pin features.

Table 2. Spread of the orientation (angles are in degree) of resultant reaction with respect to the positive *X*-axis force.

Pin flat numbers	Average orientation (θ) with range	
	Unthreaded	Threaded
0	$65.5° \pm 8°$	$23.5° \pm 44°$
1	$60° \pm 11°$	$41.5° \pm 36°$
2	$53.7° \pm 10°$	$64° \pm 16°$
3	–	$57.6° \pm 15°$
4	$46° \pm 8°$	$61.6° \pm 12°$

60° without substantial variation in resultant magnitude. In general, it can be said that the presence of flats does not greatly alter the magnitude of the resultant in-plane forces: this property seems to be dependent on thread form and weld parameters. However, the presence of flats does affect the direction of action of the resultant, narrowing the range of θ.

Effect of pin flats on tool torque and temperature

Figure 6 shows the measured torque as a function of tool rotational speed for unthreaded and threaded pins with various flat numbers. The measured torque monotonically decreases with increasing tool rotational speed for similar pin profile. Considering the unthreaded pins (Figure 6(a)), highest and lowest average torque was observed for four flatted and one flatted pin, respectively, while comparing similar welding condition until the variation of required torque becomes insignificant at 400 rev min^{-1} rotational speed. Moreover, for threaded pins, no consistent trend was observed with respect to pin flat numbers while comparing similar welding parameters, yet also variation is insignificant at highest rotational speed (400 rev min^{-1}). However, a similar study by Schneider et al. [27] revealed that increasing flat numbers on a cylindrical threaded pin resulted in a minute amplification in torque. Overall, the decrease in torque with increasing rotational speed is a common phenomenon which is due to the lessening of resistance of plasticised material around tool. The basis of this phenomenon can be elucidated by examining the process temperature. Figure 7 shows the pin peak temperature versus weld power for unthreaded (Figure 7(a)) and threaded (Figure 7(b)) pins having different flat numbers. It should be noted here that the temperature measured in the pin can be considered as an average process temperature of weld material in contact with the pin that has been found to provide reasonable representation of nugget temperature with change in welding parameters [28].

The pin peak temperature increases with increasing weld power or increasing tool rotational speed for constant welding speed in both unthreaded and threaded pins with various flat numbers. However, weld power increases significantly with increasing welding speed for a rotational speed of 240 rev min^{-1} with a minute decrease in pin peak temperature. This decrease in peak temperature is related to the fact that while weld power increases slightly with increasing welding speed at constant rev min^{-1}, unit weld energy decreases sharply [29]. A study by Reynolds et al. [29] has also shown that the temperature transient is governed by welding speed. In general, variation of flat number for unthreaded pin does not greatly affect temperature; this is mostly dominated by welding parameters. On the other hand for threaded pin, while the relationship of temperature power (Figure 7(b)), reflected in the torque-RPM plot in Figure 6(b), is not consistent with regard to flat number when all other things are constant. For example at 160 rev min^{-1} rotational speed, the pin with thread with one flat and threaded-only pin have, respectively, the highest and the lowest temperatures/power and the difference is minimised with increasing rotational speed at a welding speed of 102 mm min^{-1}. Besides, threaded-only and three flatted pin possess the highest and the lowest temperature and power at 240 rev min^{-1} and 203 mm min^{-1}, respectively. Conversely, highest weld power and temperature were evident for three flatted pin at a rotational speed of 400 rev min^{-1}.

Colour online, B/W in print

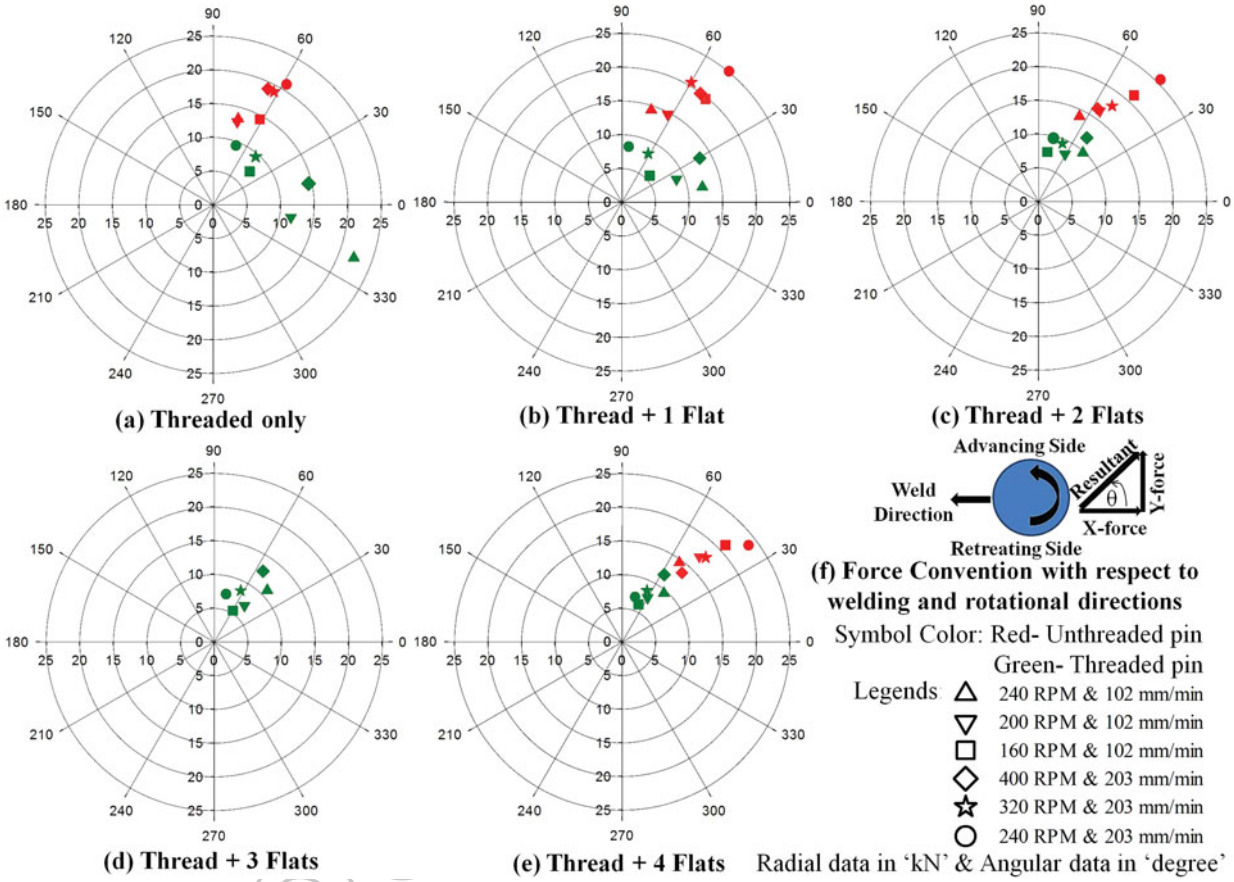

Figure 5. Polar plots of average in-plane reaction forces on tools having different flat numbers.

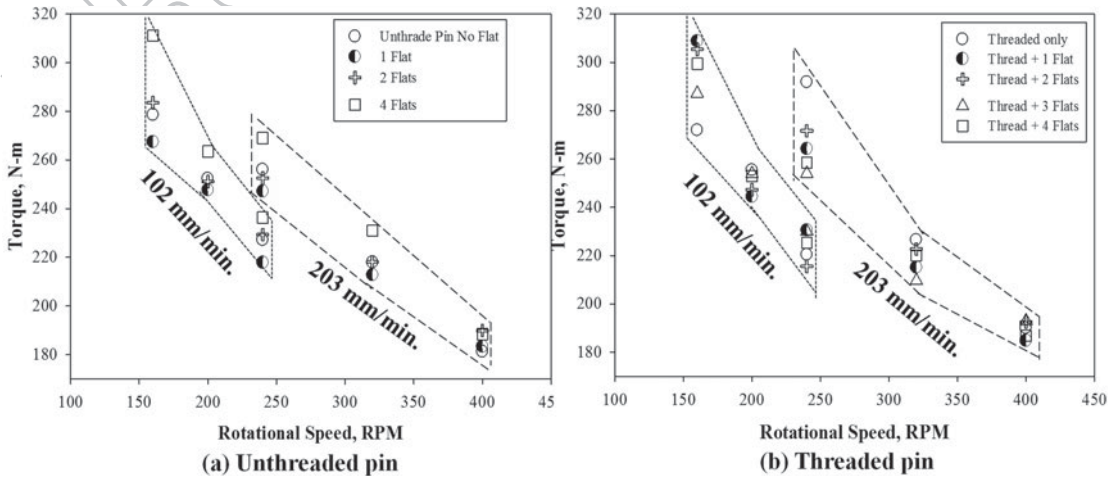

Figure 6. Tool torque as a function of rotational speed for different flat numbers.

Discussions

The experimental investigation shown in the preceding section revealed that the threaded pins with flats are capable of eliminating wormhole defects in the welds as compared to unthreaded pins regardless of the applied welding parameters. The variations in geometric features of unthreaded and threaded pins play a significant role in material movement during FSW. The behaviour of extruded and stirred material adjacent to pins can easily be understood taking into account the provision of machining flats and threads in pin.

It is obvious that mass conservation law must be satisfied to obtain defect-free welds, in which volume of the stirring pin (always circular or slightly elliptical as observed in the plan view regardless of pin geometry) is to be replaced by extruded materials along the weld seam. Therefore, machining flats in a cylindrical pin does not alter the displaced or dynamic volume of the pin rather it affects material transport phenomenon.

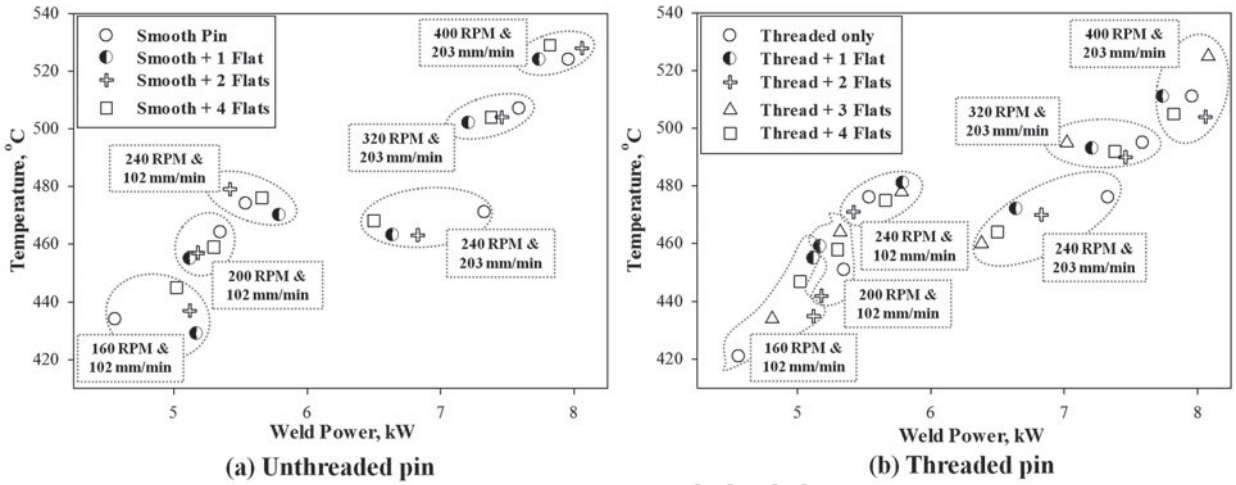

Figure 7. Pin peak temperature as a function of rotational speed for different flat numbers.

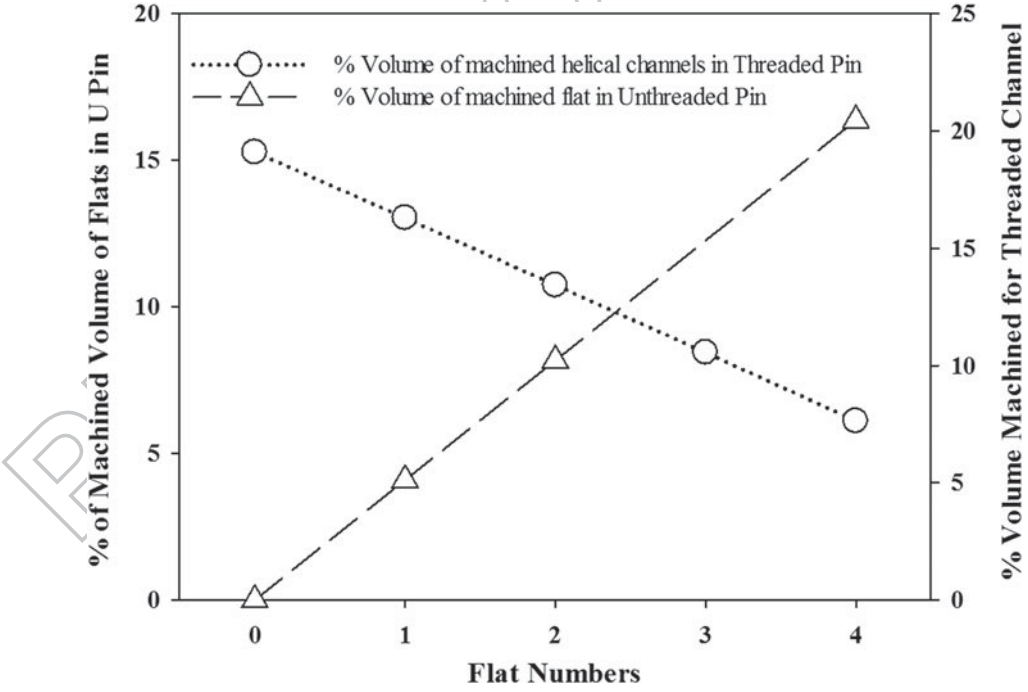

Figure 8. Per cent of volume machined from a cylindrical smooth pin for introducing flats and threads.

Figure 8 illustrates the per cent of materials machined from a smooth cylindrical pin (pin geometric dimensions considered in this investigation are mentioned in the experimental section) due to machining flats on unthreaded pin (triangular symbol) and the volume fraction of spiral channel machined in threaded pins having different flat numbers (circular symbol). From Figure 8, it is comprehensible that the volume of machined flat in the pin increases linearly with increasing flat number in unthreaded pins. During FSW, flats in pin facilitate additional material to interact – perhaps with an additional shear surface beyond the circumferential region of pin, as postulated by Schneider et al. [27] It is interesting to note similar trend of Figures 4 and 8 (considering variation of flat number for identical welding condition), where forge force requirement and machined volume of flats in pin were increased with higher flat number for unthreaded pin. This might be because of volume of processed materials surrounding tool is increased with higher flat numbers, albeit the swept volume by the pin remains constant regardless of flat numbers. It is also worth to mention here by comparing Figure 5 for unthreaded pin that the orientations of resultant reaction decrease and in-plane resultant forces increase with increasing flat numbers. These decreases in orientations of resultant are consistent with an increase in X component of the resultant which is X-axis force. Therefore, with the indication of material adhesion in flat trailing side (evident from Figure 3) it can reversibly be stated that resistance of material flow

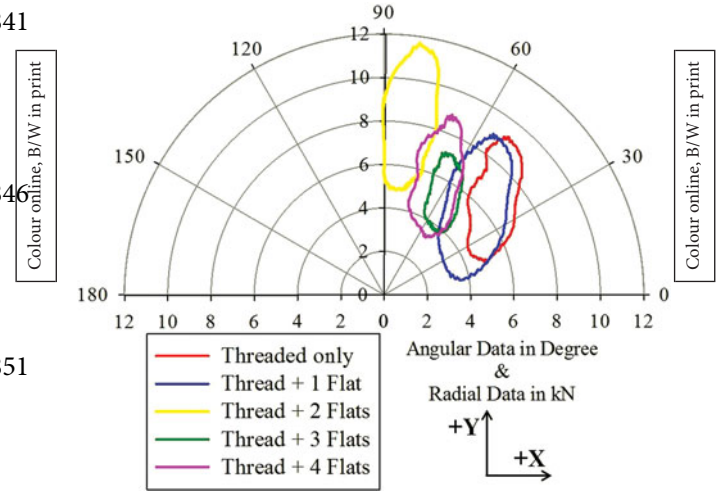

Figure 9. 'Force footprint' of in-plane forces on threaded pins with various flat numbers for one complete cycle at 240 rev min^{-1} rotational speed and 102 mm min^{-1} welding speed.

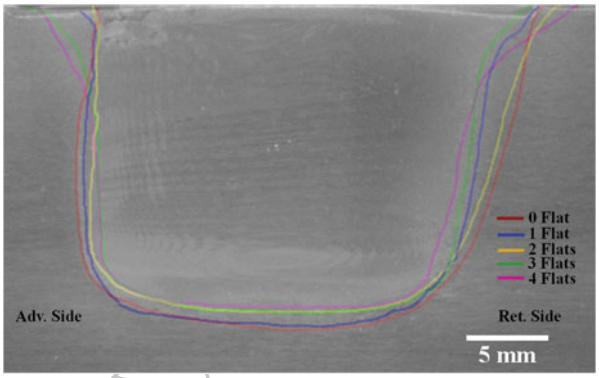

Figure 10. Nugget geometries for welds with threaded pins having various flat numbers at 240 rev min^{-1} and 102 mm min^{-1}.

increases with increasing flat numbers in unthreaded pin. This is also evident from the torque data where unthreaded pin with four flats always generated the highest torque (see Figure 6(a)).

Conversely, machining flats reduce the entrapment volume in the threaded channel, as the flat number increases (circular symbols in Figure 8) in case of threaded pins. Moreover, required forge force (see Figure 4(b)) was also found to be decreased with increasing flat numbers for similar welding condition. The effectiveness of pin thread on material transportation has been explained in the section 'Influence of flats on applied forge force and in-plane reaction forces'. However, flats interrupt the continuous downward movement of materials in the threaded channel. Therefore, gripped materials in the threaded channel of the pin are being temporarily released near flat leading edge before the adjacent material are being re-entered into the threaded channel near the trailing edge of flat during pin rotation [22]. This was also evident from the absence of material adhesion on flat surface of threaded pins (Figure 3). Moreover, the orientations of resultant reaction increase and in-plane resultant forces decrease with increasing flat numbers. These increases in orientations of resultant are also consistent with the decrease in X-axis force. Therefore, it can also be stated that increasing flat number eases the material flow around tool. These phenomena are also explained in the following paragraph with the consideration of dynamic nature of in-plane forces.

The movements of plasticised materials were found to be highly periodic during FSW [2,30,31]. Moreover, flats produce additional pulsating vibrations that may also influence the dynamic nature of feedback forces. Attempts have been made to correlate defect occurrence with the force spectra [32–34]. Figure 9 shows the polar plot of the 'force footprints' for a weld performed at 240 rev min^{-1} and 102 mm min^{-1} with threaded pin having different flat numbers. A high frequency (1000 Hz) data acquisition system was used to investigate these X-axis and Y-axis force spectra. These polar plots illustrate the periodic nature of the X-axis and Y-axis force spectra for one complete revolution of pins with different flat numbers. It was clearly observed from Figure 9 that oscillation for three flatted pin is the lowest compared to pin with other flat numbers as evident from least enclosed area within the locus of in-plane resultants as designated by the green line. Moreover, the fluctuation of Y-axis forces is more prominent than X-axis force for all the pins. Increase in tool run-out during FSW process might be attributed to such phenomenon [35]. The variations in texture of the banded microstructures suggest the occurrence of eccentric tool rotation [5]. Nevertheless, the macro-cross-sectional evaluation in this study also discloses a comprehensive influence of tool shoulder and pin feature on nugget geometry. The overlapping transverse sections in Figure 10 illustrate the effect of pin thread interruptions with flats on the thermo-mechanically affected zone (TMAZ) and nugget zone. The enclosed boundaries of different colours correspond to the area of TMAZ and nugget zone for pins having different flat numbers. For same welding condition (240 rev min^{-1} and 102 mm min^{-1}), an extended TMAZ on both advancing and retreating side near weld crown was observed for three and four flatted pins, whereas vertical sharp edge on the advancing side along with extended TMAZ near retreating side was evident for zero, one and two flatted pins. Obviously, the basin shape of nuggets is due to the shoulder induced deformation which was observed relatively more symmetrical for three and four flatted pin compared to other flat numbers including no flat. In FSW, Y force generally tries to drive the tool to move towards the advancing side. Since materials are being extruded continuously from the advancing side and higher Y force might cause lack of shoulder contact near the advancing side, thus relative colder material on advancing side

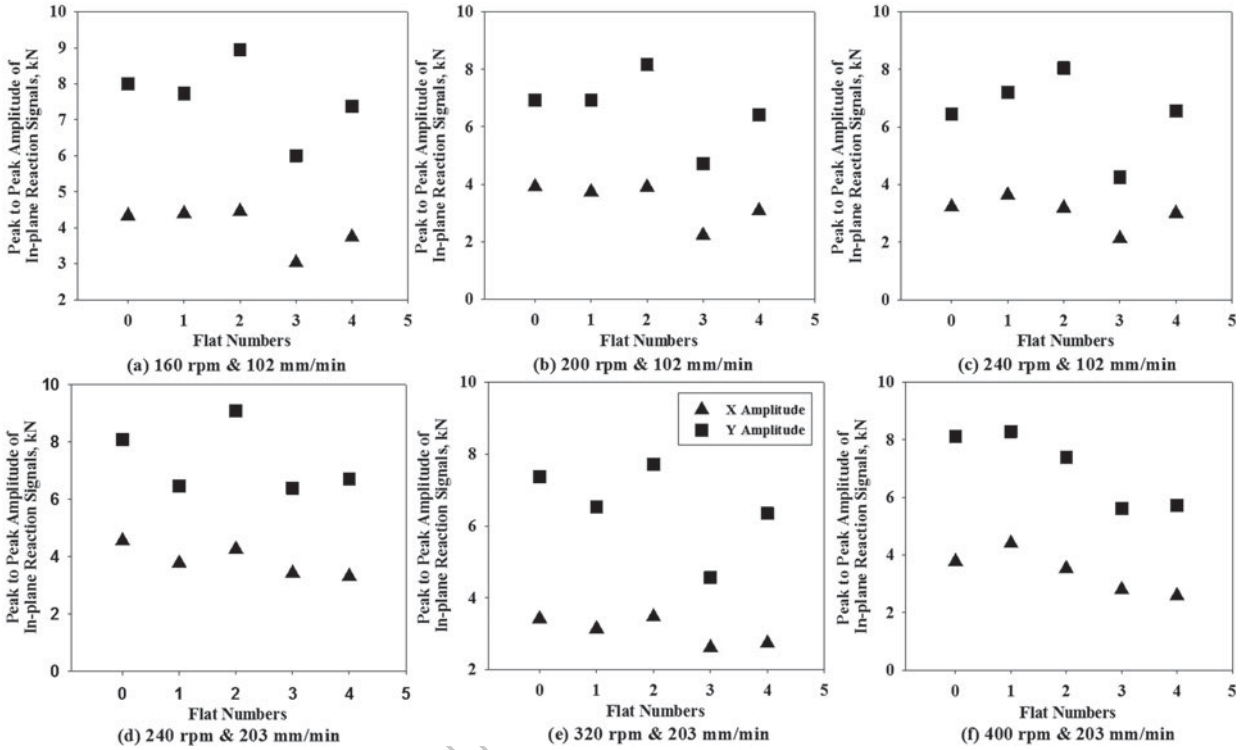

Figure 11. Peak-to-peak amplitude as a function of flat number for different welding conditions.

is opposed by pin edge subsequently resulted in a sharp edge on advancing side that coincides with vertical edge of cylindrical pin. This shear slippage constricts material movement on the advancing side; this also leads to a surface breaking defect near the weld crown on advancing side [36]. On the contrary, relatively low Y force with minute oscillatory amplitude facilitated by three and four flatted pin might cause uniform deformation of material beneath shoulder ultimately leading to symmetric basin shape nugget.

Based on the discussion of the periodic nature of force spectra along with corresponding microstructural evaluation, an effort has also been made to analyse the peak-to-peak amplitudes of the X-axis and Y-axis forces for different frequency (in this case tool rotational speed) against the flat numbers. Figure 11 presents the X-axis and Y-axis force amplitude as a function of flat number under different welding parameters. Interestingly, in most of the welding conditions it was observed that peak-to-peak amplitudes of X-axis and Y-axis force spectra were lowest for the pin with three flats. This result is more consistent in case of Y-axis force spectra. As discussed earlier, Y-axis force is related to pressure produced around pin due to material movement [30], the fluctuation with high amplitude of the spectra might be associated with irregular material movement with different tool pin having different flat numbers except that for three flats. Note that the threaded pin with three flats consistently possesses lowest peak-to-peak amplitude in force spectra as well as being most capable of producing complete defect-free welds. Therefore, it might be appropriate to conceive here: a defect in weld is most likely to occur when fluctuation of oscillation is higher albeit X-axis and Y-axis forces are not necessarily in phase.

Conclusions

The following conclusions can be drawn from this investigation:

(i) Machining of flats on a cylindrical, unthreaded pin does not eliminate wormhole defects near the weld root under the conditions examined in this study. However, flats on unthreaded pins do appear to facilitate material flow around the pin as the observed defect may be less localised to the advancing side with increased flat number.

(ii) Threads in pins significantly improve downward material movement by eliminating obvious wormhole defects as compared to unthreaded pins with/without flats.

(iii) Flats in threaded pin also affect process response variables in FSW and alter the deformation of processed materials. This may be due to the entrapment of weld material in the threaded channel and subsequent releasing near flats continuously during tool rotation and traverse. Moreover, three flatted pin effectively eliminates both wormhole and surface breaking defects with lowest in-plane reaction forces for the examined conditions.

(iv) The introduction of threads and flats reduced in-plane forces. Moreover, flats in pin affect the distribution of the direction of in-plane resultant forces.

While flat number increases, range of orientation of resultant forces decreases for threaded pin; however, this range does not alter much for unthreaded pin.

(v) Amplitude of the oscillation of feedback force signal is observed to be the lowest for the pin having three flats. This is associated with minor or even no defects in the welds. Significantly, lower variation in force oscillation for three flatted pin perhaps leading to better fatigue life.

Acknowledgements

The authors thank Mr. Daniel Wilhelm, Associate Engineer, Department of Mechanical Engineering, University of South Carolina, Columbia, SC, USA for his help in manufacturing pins and preparing the weld joints.

Disclosure statement

No potential conflict of interest was reported by the authors.

Funding

The authors acknowledge the financial support of the Center for Friction Stir Processing which is a National Science Foundation I/UCRC (NSF I/UCRC) supported by Grant no. EEC-0437341.

References

[1] Thomas W, Nicholas E, Needham J, et al. GB Patent Application no. 9125978-9; 1991.
[2] Colligan K. Material flow behaviour during friction welding of aluminum. Weld J. 1999;75(7):229s–237s.
[3] Schneider J, Nunes A Jr. Characterization of plastic flow and resulting microtextures in a friction stir weld. Metall Mater Trans B. 2004;35(4):777–783.
[4] Zhao Y-H, Lin S-B, Wu L, et al. The influence of pin geometry on bonding and mechanical properties in friction stir weld 2014 Al alloy. Mater Lett. 2005;59(23):2948–2952.
[5] Fonda R, Reynolds A, Feng C, et al. Material flow in friction stir welds. Metall Mater Trans A. 2013;44(1):337–344.
[6] Burford D, Tweedy B, Widener C. Influence of shoulder configuration and geometric features on FSW track properties. Proceedings of the Sixth International Symposium on Friction Stir Welding; 2006. p. 10–13.
[7] Dawes C, Thomas W. Development of improved tool designs for friction stir welding of aluminium. 1st International Symposium on Friction Stir Welding; 1999. p. 1–10.
[8] Zettler R, Lomolino S, dos Santos JF. A Study of Material Flow in FSW of AA2024-T351 and AA 6056-T4 Alloys. Proceedings of the Fifth International Conference on Friction Stir Welding; 2004 Sept 14–16; Metz;2004; TWI, paper on CD.
[9] Ahmed M, Wynne B, Rainforth W, et al. Through-thickness crystallographic texture of stationary shoulder friction stir welded aluminium. Scr Mater. 2011;64(1):45–48.
[10] Davies P, Wynne B, Rainforth W, et al. Development of microstructure and crystallographic texture during stationary shoulder friction stir welding of Ti-6Al-4V. Metall Mater Trans A. 2011;42(8):2278–2289.
[11] Ji S, Meng X, Liu J, et al. Formation and mechanical properties of stationary shoulder friction stir welded 6005A-T6 aluminum alloy. Mater Des (1980–2015). 2014;62:113–117.
[12] Russell MJ, Blignault C. Recent developments in friction stir welding of Ti alloys. Proceedings of the Sixth International Symposium on Friction Stir Welding, 2006 Oct 10–13; Saint-Sauveur; 2006, CD-ROM.
[13] Mishra RS, Ma Z. Friction stir welding and processing. Mater Sci Eng R Rep. 2005;50(1):1–78.
[14] Hattingh D, Blignault C, Van Niekerk T, et al. Characterization of the influences of FSW tool geometry on welding forces and weld tensile strength using an instrumented tool. J Mater Process Technol. 2008;203(1):46–57.
[15] Elangovan K, Balasubramanian V. Influences of pin profile and rotational speed of the tool on the formation of friction stir processing zone in AA2219 aluminium alloy. Mater Sci Eng A. 2007;459(1):7–18.
[16] Fujii H, Cui L, Maeda M, et al. Effect of tool shape on mechanical properties and microstructure of friction stir welded aluminum alloys. Mater Sci Eng A. 2006;419(1):25–31.
[17] Mahmoud E, Takahashi M, Shibayanagi T, et al. Effect of friction stir processing tool probe on fabrication of SiC particle reinforced composite on aluminium surface. Sci Technol Welding Joining. 2009;14(5):413–425.
[18] Palanivel R, Koshy Mathews P, Murugan N, et al. Effect of tool rotational speed and pin profile on microstructure and tensile strength of dissimilar friction stir welded AA5083-H111 and AA6351-T6 aluminum alloys. Mater Des. 2012;40:7–16.
[19] Aissani M, Gachi S, Boubenider F, et al. Design and optimization of friction stir welding tool. Mater Manuf Process. 2010;25(11):1199–1205.
[20] Jamshidi Aval H, Serajzadeh S, Kokabi A, et al. Effect of tool geometry on mechanical and microstructural behaviours in dissimilar friction stir welding of AA 5086-AA 6061. Sci Technol Welding Joining. 2011;16(7):597–604.
[21] Thomas WM, Nicholas ED, Smith SD. Friction Stir Welding-Tool Developments. Aluminum 2001-Proceedings of the TMS 2001; 2001 Feb 11–15; New Orleans, LA; 2001. p. 213–224.
[22] Prangnell P, Heason C. Grain structure formation during friction stir welding observed by the 'stop action technique'. Acta Mater. 2005;53(11):3179–3192.
[23] Colegrove P, Shercliff H. Development of trivex friction stir welding tool part 2–three-dimensional flow modelling. Sci Technol Welding Joining. 2004;9(4):352–361.
[24] Trimble D, Monaghan J, O'Donnell G. Force generation during friction stir welding of AA2024-T3. CIRP AnnManuf Technol. 2012;61(1):9–12.
[25] Balasubramanian N, Gattu B, Mishra RS. Process forces during friction stir welding of aluminium alloys. Sci Technol Welding Joining. 2009;14(2):141–145.
[26] Reza-E-Rabby M, Reynolds AP. Effect of tool pin thread forms on friction stir weldability of different aluminum alloys. Procedia Eng. 2014;90:637–642.
[27] Schneider J, Brooke S, Nunes AC Jr. Material flow modification in a FSW through introduction of flats. Metall Mater Trans B. 2016;47(1):720–730.
[28] Brown R, Tang W, Reynolds A. Multi-pass friction stir welding in alloy 7050-T7451: effects on weld response

variables and on weld properties. Mater Sci Eng A. 2009;513–514:115–121.
[29] Reynolds A, Tang W, Khandkar Z, et al. Relationships between weld parameters, hardness distribution and temperature history in alloy 7050 friction stir welds. Sci Technol Welding Joining. 2005;10(2):190–199.
[30] Boldsaikhan E, Burford DA, Gimenez P. Effect of plasticized material flow on the tool feedback forces during friction stir welding. Proc. Conf. On 'Friction stir welding and processing VI', San Francisco, CA; 2011. p. 335–343.
[31] Reynolds A. Flow visualization and simulation in FSW. Scr Mater. 2008;58(5):338–342.
[32] Burford D, Britos PG, Boldsaikhan E, et al. Evaluation of friction stir weld process and properties for aerospace application: e-NDE for friction stir processes. National Institute for Aviation Research, Wichita State University, Wichita, KS FAA Joint Advanced Materials & Structures (JAMS) 6th Annual Technical Review Meeting; 2010.
[33] Crawford R, Cook G, Strauss A, et al. Experimental defect analysis and force prediction simulation of high weld pitch friction stir welding. Sci Technol Welding Joining. 2006;11(6):657–665.
[34] Doude H, Schneider J, Patton B, et al. Optimizing weld quality of a friction stir welded aluminum alloy. J Mater Process Technol. 2015;222;188–196.
[35] Yan J, Sutton M, Reynolds A. Processing and banding in AA2524 and AA2024 friction stir welding. Sci Technol Welding Joining. 2007;12(5):390–401.
[36] Doude HR, Schneider JA, Nunes AC Jr. Influence of the tool shoulder contact conditions on the material flow during friction stir welding. Metall Mater Trans A. 2014;45(10):4411–4422.